


REGULAR PAPER

Research on parameter matching characteristics of pneumatic launch systems based on co-simulation

Z. Zhang , Y. Peng, X. Wei, H. Nie, H. Chen and L. Li

Key Laboratory of Fundamental Science for National Defense-Advanced, Design Technology of Flight Vehicle, Nanjing University of Aeronautics and Astronautics, Nanjing, Jiangsu, China and State Key Laboratory of Mechanics and Control of Mechanical Structures, Nanjing, Jiangsu, 210016, China
E-mail: wei_xiaohui@nuaa.edu.cn

Received: 10 March 2021; **Revised:** 6 July 2021; **Accepted:** 7 July 2021

Keywords: Pneumatic launch; Co-simulation; Dynamics analysis; Matching envelope; Optimisation design

Abstract

Pneumatic launch systems for Unmanned Aerial Vehicles (UAVs), including mechanical and pneumatic systems, are complex and non-linear. They are subjected to system parameters during launch, which leads to difficulty in engineering research analysis. For example, the mismatch between the UAV parameters and the parameter design indices of the launch system as well as the unclear design indices of the launching speed and overload of UAVs have a great impact on launch safety. Considering this situation, some studies are presented in this paper. Taking the pneumatic launch system as a research object, a pneumatic launcher dynamic simulation model is built based on co-simulation considering the coupling characteristics of the mechanical structure and transmission system. Its accuracy was verified by laboratory test results. Based on this model, the paper shows the effects of the key parameters, including the mass of the UAV, cylinder volume, pressure and moment of inertia of the pulley block, on the performance of the dynamic characteristics of the launch process. Then, a method for matching the parameter characteristics between the UAV and launch system based on batch simulation is proposed. The set of matching parameter values of the UAV and launch system that satisfy the launch take-off safety criteria are calculated. Finally, the influence of the system parameters of the launch process on the launch performance was analysed in detail, and the design optimised. Meaningful conclusions were obtained. The analysis method and its results can provide a reference for engineering and theoretical research and development of pneumatic launch systems.

Nomenclature

a	launch accelerated speed of the UAV
A_1	area of cylinder with rod cavity
A_2	area of cylinder without rod cavity
C_D	drag coefficient
C_L	lift coefficient
d_c	cylinder piston rod diameter
D	force of the aerodynamic drag
D_c	cylinder outer diameter
f_h	friction of the movable pulley assembly Force
F_f	friction between the trolley and the sliding rail
F_i	force of the i – th wire rope in the pulley block
F_t	force of rope traction
F_z	load force of the cylinder piston rod
g	acceleration of gravity
H	height of the mass from the frame
I_p	inertia of the pulley
J_c	pulley block moment of inertia

L	force of the aerodynamic lift
m_h	mass of the movable pulley assembly
m_p	mass of a single pulley
m_Z	total mass of the trolley and the UAV
M	gaseous mass
n_1	total number of design variables
Q_m	Gas mass flow rate
r_c	radius of the bearing
r_h	radius of the pulley
R	gas constant
S	area of the wing
S_c	cylinder exhaust area
S_i	sensitivity of each design variable change
S_{ref}	aircraft wing area
S_{ri}	percentage of sensitivity
S_s	cylinder actuation stroke
n_h	pulley block magnification
P	air source pressure
P_{10}	initial pressure of the air intake cavity
P_{20}	initial pressure of the gas cavity
t	time
t_1	landing time of the mass
T	degree Kelvin
T_{10}	initial temperature of the air intake cavity
T_{20}	initial temperature of the gas cavity
T_e	force of the UAV engine thrust
T_s	temperature
v	speed of UAV
v_0	launch velocity
v_{max}	maximum speed of the UAV launch
v_{min}	minimum speed of the UAV launch
V	cylinder volume
V_{10}	initial volume of the air intake cavity
V_{20}	initial volume of the gas cavity
x	displacement of the trolley and the UAV
x_1	displacement of the cylinder piston rod
X	launch distance of the mass
X_s	cylinder stroke at the moment
X_{10}	length of the cylinder with rod cavity clearance
X_{20}	cylinder without rod cavity clearance length
α	installation angle of the UAV
γ	launch angle of the launch device
ρ_{air}	air density
ρ_{gas}	gas density
μ	friction coefficient of the system
μ_1	friction factor of the pulley bearing rotation
μ_h	friction factor of the moving pulley block
κ	ratio of specific heat
θ	launch angle

1.0 Introduction

To reduce the requirements of the launch process of UAVs on site, modern UAVs mostly adopt pneumatic launching systems that can accelerate the take-off process in a limited space and very short time. However, due to this short-distance take-off and instantaneous operation, the number of cases of launch

failure has increased during recent years. According to statistical data from the Unmanned Aircraft System Incident Report (UASAR) by the US Department of Defense [1], the number of accidents caused by UAV launch systems is enormous.

Pneumatic launch systems are complex and highly non-linear systems that involve mechanisms, electricity and pneumatics and can be influenced by various factors [2]. Therefore, it is very challenging to analyse the dynamic characteristics of the UAV pneumatic launch process. Although many scholars have performed many studies on the dynamics of UAV launch systems, most of these have used numerical simulations to construct mathematical models of the UAV launching process followed by analysis and optimisation of the design on this basis. Kondratiuk [3] proposed a novel concept for a launcher powered by kinetic energy stored in a rotary wheel driven by an electric motor, and performed analysis. Jastrzebski [4] performed a theoretical analysis using a mathematical model of the airstream flow of a pneumatic launcher and compared the results obtained from the simulations with experiment. Szczepaniak [5] analysed the influence of the flow characteristics of the pneumatic distributor on the pneumatic launcher. Based on Computational Fluid Dynamics (CFD) simulation and test calculations of the maximum gas flow rate during the launch process, Huang [6] established two dynamic models for a UAV launch system based on the Lagrange equation and MSC. Automatic Dynamic Analysis of Mechanical Systems (ADAMS) and performed a detailed analysis based on the experimental results. Liu [7] established a mathematical model for a pneumatic launch system based on the power bond diagram and studied the influence of different parameters on the performance of the launch system. Lu [8], based on the closed vector loop method and force balance equation, derived a solution for the dynamics of a mathematical model for a wedge-shaped launcher and optimised it by using the multi-objective genetic algorithm.

Because the dynamics of pneumatic launch systems represents a complex non-linear problem including the mechanical structure and pneumatic drive system, the traditional dynamic modelling method is mostly based on theoretical formulas to establish and simulate the dynamics model, thus relying too heavily on mathematical models and being unable to reflect the real process of UAV launch. Co-simulation can be effectively applied to pneumatic launch systems based on the interaction between the mechanical and pneumatic transmission systems in the problem [9,10] by integrating the two corresponding simulation models. This approach can thus obtain a more realistic UAV pneumatic launch system dynamics model to analyse this interaction.

Moreover, studies in this field have mainly focused on model building, dynamic analysis and optimisation but have not included research on the parameter matching characteristics of UAVs with launch systems based on pneumatic launching. In the pneumatic launch process, changes in system parameters such as the pressure, volume of gas cylinder and moment of inertia of the pulley block are subjected to the dynamic performance of the launch process. Degrading these parameter may also reduce the take-off speed of the UAV, causing it to crash, whereas enhancing them may result in an overload on the UAV and damage its body structure or flight control equipment. These parameters can only ensure safe launching when they satisfy the mutual matching relationship. Therefore, to improve the success rate of UAV launches, it is of great significance to conduct in-depth research on the key parameters that affect the launch and the parameter matching characteristics of pneumatic launch systems with UAVs. In recent years, some scholars have included parameter matching characteristics in their research and expanded the related field of dynamic parameter inversion [11]. Liu established a mathematical model for carrier-based aircraft catapult take-off considering the complex environment of take-off from a ship surface and calculated the set of main aircraft and ship parameter matching values that satisfied the safety criteria for catapult take-off [12].

The parameter matching characteristic between the UAV system and launch system is one of the most critical issues in the design phase of the overall plan for UAV launching. In this paper, a complete and accurate dynamic model for pneumatic launches is established based on multi-disciplinary co-simulation, considering the coupling characteristics of the system. We analyse the impact of the key parameters on the safety performance of the launch process in detail. The speed and overload dynamic characteristics of the UAV during launch under different parameters are analysed based on batch simulation, thus revealing the effects of the key parameters, including the mass of the UAV, moment of inertia

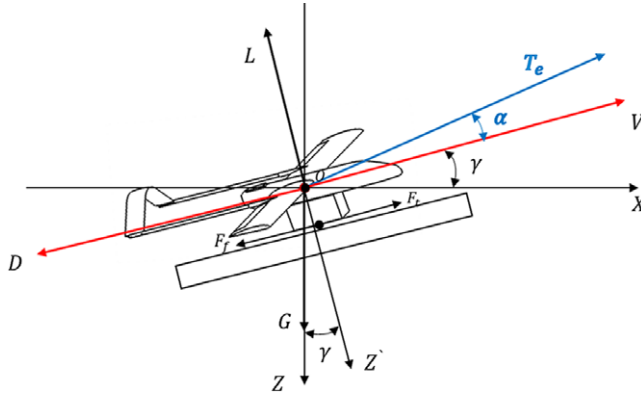


Figure 1. Force analysis diagram of the UAV acceleration process.

of the pulley block and working pressure, on the launch performance. Finally, the paper summarises the parameter matching characteristics between the UAV and launch systems. The research results presented herein provide an important theoretical reference for engineering, research and development of UAV pneumatic launch systems.

2.0 Modelling the Pneumatic Launch Process Dynamics

2.1 Kinematics equation of UAV launch process

From a kinematic viewpoint, the launch operation can be described as accelerating the UAV and trolley along a launch frame under the action of the engine thrust and traction force of a traction rope while overcoming friction, aerodynamic forces including lift and drag, and the force of gravity. The traction force is provided by the action of compressed gas on the cylinder piston rod and transmitted by an accelerating pulley block. A schematic diagram of the forces during the launch process is shown in Fig. 1.

Considering the UAV and trolley as point masses, one can derive the equation of motion of the UAV acceleration process as

$$m_z \frac{d^2x}{dt^2} = F_t + T_e \cos(\alpha) - (m_z g - L \cos(\gamma)) \sin \gamma - F_f - D \tag{1}$$

where F_t is the traction in the rope, T_e is the UAV engine thrust, L is the aerodynamic lift, D is the aerodynamic drag, F_f is the friction between the trolley and the sliding rail, m_z is the total mass of the trolley and the UAV, x is the displacement of the trolley and the UAV, α is the installation angle of the UAV and γ is the launch angle of the device.

The aerodynamic force and friction between the trolley and sliding rail of the launcher can be calculated as:

$$L = \frac{1}{2} S C_L \rho v^2 \tag{2}$$

$$D = \frac{1}{2} S C_D \rho v^2 \tag{3}$$

$$F_f = \mu(m_z g \cos \gamma - L) \tag{4}$$

where S is the wing area, C_L is the lift coefficient, C_D is the drag coefficient, ρ is the density of air, v is the speed of the UAV and μ is the friction coefficient of the system.

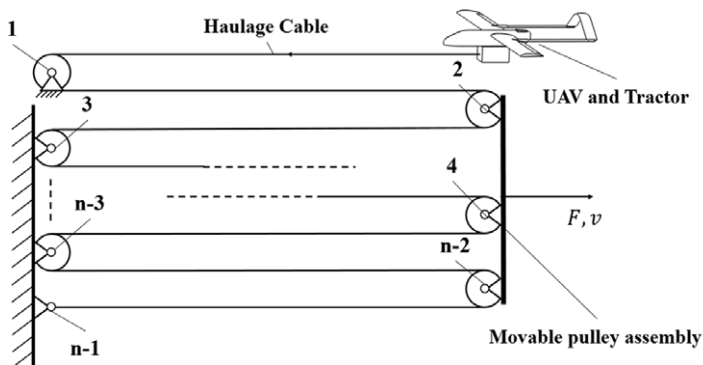


Figure 2. Schematic diagram of the accelerating pulley block.

2.2 Dynamic model of the accelerating pulley block

As shown in Fig. 2, the load force on the cylinder piston rod is transmitted to supply the driving force on the movable pulley assembly, UAV and pulley during the launch process. The accelerating pulley block, which includes a fixed pulley and a movable pulley [13], increases the pneumatic launch speed and stroke of the UAV because the stroke and end speed of the cylinder as an actuator are limited. The free end of the steel wire rope is connected to the pulley, while the other end wraps around the reversing fixed pulley, which is wound with the movable and fixed pulleys in turn, while the end is fixed.

When the cylinder starts to act and provides a driving force for the launch, the accelerating pulley block acts to increase the speed and distance. Simultaneously, the transmission of the driving force is completed. To analyse the relationship between the traction force of the rope acting on the UAV and pulley and the driving force of the cylinder, the movable pulley assembly is considered as the moving body, and several reasonable assumptions should be made before the dynamic analysis:

- (1) The traction rope does not deform during the launch process, and its own weight and rigid resistance can be ignored;
- (2) The rotation speed of the pulley at a given time is identical to the linear speed of the wire rope contact point;
- (3) The moving pulley assembly and cylinder piston rod move synchronously; i.e., their speeds are identical.

The dynamic equation for the moving pulley group can thus be expressed as

$$F_z = F_t + \sum_{i=1}^{n_h-1} F_i + f_h + m_h \frac{d^2s}{dt^2} \tag{5}$$

where F_z is the load force of the cylinder piston rod, F_t is the rope traction, x_1 is the displacement of the movable pulley assembly and the cylinder piston rod, F_i is the force of the i -th wire rope in the pulley block, m_h is the mass of the movable pulley assembly, f_h is the friction of the movable pulley assembly force and n_h is the pulley block multiplication factor.

The forces on the winding-in side and winding-out side of the same pulley are not identical, being related as

$$F_i = F_{i+1} + f_{hi} \tag{6}$$

where $f_{hi}(i = 1, 2, \dots, n - 1)$ is the friction force of the rope on the i -th pulley. When $i = 1$, $F_0 = F_t$, one has

$$F_1 = F_t + f_{h1} \tag{7}$$

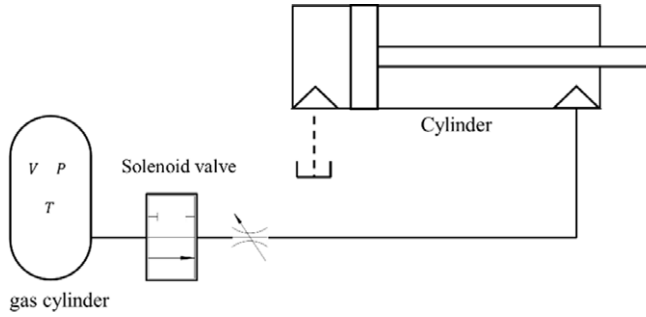


Figure 3. Schematic diagram of the gas cylinder deflation model.

According to the preceding analysis, the driving force for the rotation of the pulley is generated by the friction between the wheel and the rope. The rotation of the pulley generates a torque. Combined with the friction at the pulley bearing, the following can be obtained:

$$F_z = K_1 F_t + K_2 \frac{d^2x}{dt^2} + \mu_h m_h g \tag{8}$$

$$K_1 = n + \frac{\mu_1 r_c}{r_h - \mu_1 r_c} \sum_{i=0}^{n-2} (n - 1 - i) \left(1 + \frac{\mu_1 r_c}{r_h - \mu_1 r_c}\right)^i \tag{9}$$

$$K_2 = m_h + \frac{n I_p}{r_h (r_h - \mu_1 r_c)} \sum_{i=0}^{n-2} (n - 1 - i) \left(1 + \frac{\mu_1 r_c}{r_h - \mu_1 r_c}\right)^i \tag{10}$$

$$I_p = m_p (r_n^2 - r_c^2) \tag{11}$$

where μ_h is the friction factor of the moving pulley block, μ_1 is the friction factor corresponding to the rotation of the pulley bearing, I_p is the inertia of the pulley, r_h is the radius of the pulley, r_c is the radius of the bearing and m_p is the mass of a single pulley.

2.3 Dynamic analysis of the pneumatic transmission system

In a pneumatic launch, the pneumatic system mainly provides energy to speed up the UAV. The entire working process is a short-term thermodynamic process that is both complex and diverse. To facilitate this theoretical analysis, the gas is considered to be ideal. The process is considered to be quasi-static and adiabatic. Therefore, the work done by the pneumatic system during the entire launch process can be divided into the dynamic process of constant-volume cylinder deflation and high-speed cylinder movement, thus the mathematical model for the launch process can be obtained.

(1) Mathematical model of the gas cylinder deflation process

The gas cylinder deflation diagram is shown in Fig. 3.

We assume that the volume of the gas cylinder is V and that the container has been filled with compressed air before deflation, and use the adiabatic venting energy equation for a limited volume [14–16],

$$-\kappa RT dM = \kappa p dV = V dp \tag{12}$$

For the gas cylinder, $dV = 0$ and $dM = Q_m dt$. The equation for the change in pressure during the gas cylinder deflation process with time can be expressed as

$$dt = \frac{dM}{Q_m} = -\frac{V dp}{\kappa RT Q_m} \tag{13}$$

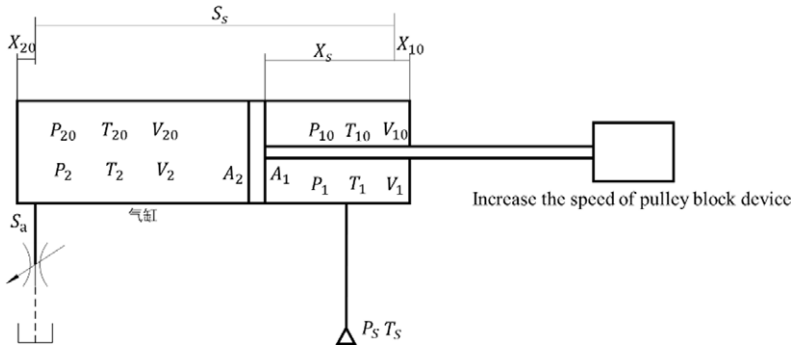


Figure 4. Schematic diagram of the cylinder operating process.

$$\frac{dp}{dt} = -\frac{\kappa RT Q_m}{V} \tag{14}$$

where κ is the ratio of specific heats, R is the gas constant, T is temperature in Kelvin, M is the gaseous mass, ρ is the gas density, V is the cylinder volume, Q_m is the gas mass flow rate and t is time.

(2) Mathematical model of the cylinder work process

Figure 4 shows a schematic diagram of the work process of the cylinder. X_{10} is the length of the cylinder with rod cavity clearance, X_{20} is the cylinder without rod cavity clearance length, S_s is the cylinder actuation stroke, X_s is the cylinder stroke at moment t and S_a is the cylinder exhaust area.

Suppose that P_s is the air source pressure, T_s is the temperature, $A_1, P_{10}, T_{10}, V_{10}$ and $A_2, P_{20}, T_{20}, V_{20}$ are the area, initial pressure, temperature and volume of both sides of the cylinder; T_1, P_1, V_1 and T_2, P_2, V_2 are the parameters at moment t .

According to the relevant theory of a pneumatic transmission system, the equation for the change in the pressure in the cylinder rod cavity can be obtained as

$$\frac{dp_1}{dt} = \frac{\kappa RT_s Q_{m1}}{V_1} - \frac{\kappa p_1}{V_1} \frac{dV_1}{dt} \tag{15}$$

The equation for the pressure change in the rodless cavity of the cylinder can be expressed as

$$\frac{dp_2}{dt} = \frac{\kappa p_2}{(S_s + X_{20} - X_s)} \frac{dX}{dt} - \frac{\kappa RT_2 Q_{m2}}{A_2(S_s + X_{20} - X_s)} \tag{16}$$

3.0 Analysis of Pneumatic UAV Launch and Verification by Testing

The pneumatic launch process for UAVs is a nonlinear dynamics problem including mechanical systems and pneumatic transmission coupling. Due to the complexity of the operating process of the system, the accuracy of the corresponding dynamic characteristic parameters cannot be guaranteed by only calculation and analysis. The dynamic characteristics of the UAV pneumatic launch process are thus studied experimentally to obtain an accurate and reliable simulation model and thus enable deep study of the UAV pneumatic launch process.

3.1 Experimental methods

Based on a virtual prototype of the pneumatic launch system, test pieces of the parts were processed and assembled. A generator powered the entire device, and air compressors stored energy for gas cylinders mounted outside the launcher. A cylinder was installed into the device to perform the pull-back action. A five-fold accelerating pulley block device was used to increase the speed and distance. The pneumatic

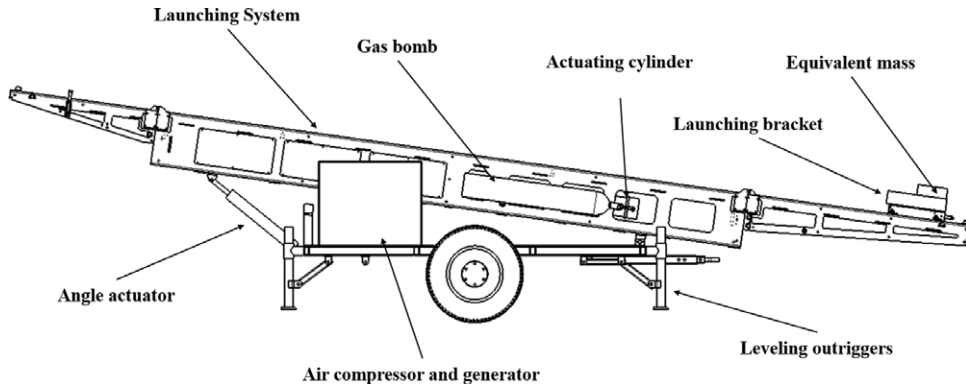


Figure 5. Pneumatic catapult structure diagram.



Figure 6. Pneumatic launch test chart.

system was built, and a Programmable Logic Controller (PLC) was applied for integrated control of signal collection. During the pneumatic launch, the pressure signal in the pneumatic transmission system was collected by the PLC, and the air compressor was controlled to store the energy in the storage cylinder. When the set working pressure was reached, the pneumatic servo valve was controlled to open to start the cylinder operation and perform the ground test of the pneumatic launch process. The pneumatic launch test is shown in Figs. 5 and 6.

The ground test of the pneumatic launch system was performed without aerodynamic loads. Equivalent mass blocks were used to simulate UAVs of different masses. By measuring the launch device angle, the height of the mass as it leaves the device and location of the mass block, we calculated the maximum launch speed that the launch device could achieve. The mass of the UAV and pneumatic parameters were adjusted by changing the mass and air compressor parameters to satisfy the index requirements. Several tests were conducted, and the influence of different parameters on the dynamic characteristics of the pneumatic launch device was studied.

The core formula for the experimental system measurements can be obtained as follows:

$$\begin{cases} H = v_0 \cdot t_1 \cdot \sin \theta - \frac{1}{2} g t_1^2 \\ X = v_0 \cdot t_1 \cos \theta \end{cases} \quad (17)$$

Table 1. Comparison of simulation and test results

Working condition	Launch mass (kg)	Pressure (MPa)	Test speed (m/s)	Simulation speed (m/s)	Error (%)
1	20	0.39	25.7	26.86	4.5
2	20	0.59	33.1	34.65	4.6
3	30	0.59	28.9	29.57	2.3

The launch time can be expressed as

$$t_1 = \sqrt{\frac{2(X \cdot \tan \theta - H)}{g}} \quad (18)$$

Thus, the maximum launch velocity can be expressed as

$$v_0 = \frac{X\sqrt{g}}{\cos \theta \cdot \sqrt{2(X \cdot \tan \theta - H)}} \quad (19)$$

where H is the height of the mass from the frame, g is the acceleration due to gravity, θ is the launch angle, X is the distance between the landing point of the mass and the frame, t_1 is the landing time of the mass and v_0 is the launch velocity.

3.2 Model verification

Three sets of experiments were performed using the pneumatic launcher, and the test results were compared with the simulation results. The parameters studied were as follows: UAV installation angle $\alpha = 2^\circ$, launch angle $\gamma = 8^\circ$, cylinder outer diameter $D_c = 250\text{mm}$, cylinder piston rod diameter $d_c = 50\text{mm}$, cylinder volume $V = 80\text{L}$, inflation pressure $P = 0.39\text{MPa}$, pulley mass $m_c = 8\text{kg}$, pulley block moment of inertia $J_c = 0.02\text{kg}\cdot\text{m}^2$ and friction coefficient $\mu = 0.01$.

The comparison results are presented in Table 1.

As shown in Table 1, the theoretical results agree well with the test results. The errors are all within 5%, providing that the established dynamic model is relatively accurate and can be used for simulation analysis of UAV pneumatic launch dynamics.

4.0 Effects and Sensitivity Analysis of Pneumatic Launch System Performance Parameters

In the process of a pneumatic UAV launch, the take-off speed and launch overload are the two most important performance parameters determining whether the UAV can complete the launch safely and stably. Therefore, based on a dynamic model using co-simulation in LMS Virtual.Lab Motion [17] and AMESim [18], the effects of some key parameters on the launch performance were scrutinised.

In LMS Virtual.Lab Motion, the motion relationship and contact relationship of each structure involved in the UAV launch process were established, the aerodynamic force of the UAV was defined based on LMS Imagine.Lab Amesim and the pneumatic subsystem of the UAV pneumatic launch system was built. The model uses the interface module provided by Amesim to perform pneumatic–mechanical co-simulation and analyse the effects of various parameters such as the UAV mass, take-off angle, pulley inertia, cylinder pressure, cylinder volume and cylinder effective area on the dynamic characteristics of the UAV launch process.

4.1 Effect of cylinder pressure

The working pressure of the gas cylinder of the pneumatic transmission system affects the dynamic characteristics of the launch system. To analyse the influence of the pneumatic transmission system-related

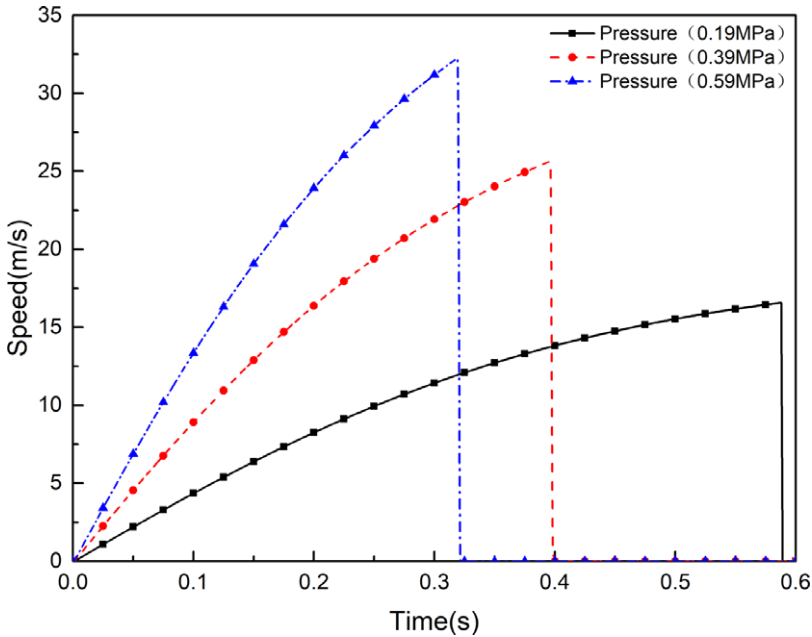


Figure 7. The influence of the air tank pressure on the take-off speed.

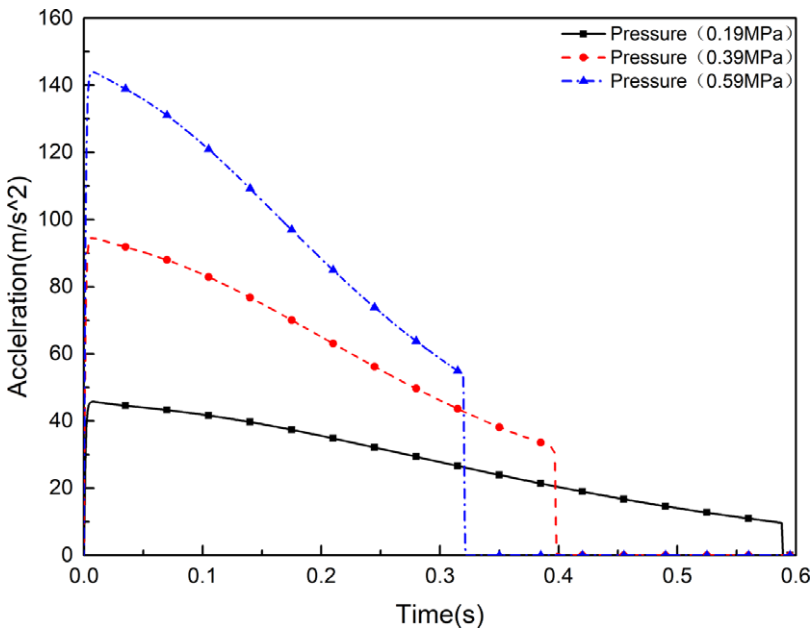


Figure 8. The influence of the air tank pressure on the take-off overload.

parameters on the launch performance, the working pressure of the gas cylinder was set to 0.19MPa, 0.39MPa and 0.59MPa. Other system parameters were taken as fixed values, specifically: the mass of UAV was 20kg, the launch angle was 8°, the pulley block moment of inertia was 0.02kg·m², the cylinder volume was 80L and the cylinder action area was 0.042m². We performed the simulation using the co-simulation model. The speed and acceleration results are shown in Figs. 7 and 8.

Table 2. Influence of cylinder pressure

Response parameter	Cylinder pressure		
	0.19MPa	0.59MPa	Increase
Maximum launch speed	16.6m/s	32.2m/s	94%
Maximum launch overload	4.6g	14.4g	213%

Table 3. Influence of other parameters

Response parameter	UAV mass		
	10kg	30kg	Increase
Maximum launch speed	29.8m/s	22.8m/s	-23.5%
Maximum launch overload	12.7g	7.5g	-41%
Influence parameter	Launch angle		
Value	1°	15°	Growth ratio
Maximum launch speed	25.8m/s	25.4m/s	-1.5%
Maximum launch overload	9.6g	9.4g	-2%
Response parameter	Moment of inertia		
Value	0.02 kg · m ²	0.12 kg · m ²	Increase
Maximum launch speed	25.6m/s	16.5m/s	-35.5%
Maximum launch overload	9.5g	4.1g	-56.8%
Response parameter	Cylinder volume		
Value	40L	120L	Increase
Maximum launch speed	25.8m/s	27.6m/s	6.9%
Maximum launch overload	9.6g	9.6g	0%
Influence parameter	Cylinder effective area		
Value	0.03 m ²	0.077 m ²	Increase
Maximum launch speed	22.1 m/s	28.9 m/s	30.7%
Maximum launch overload	5.9 g	15.8 g	167.7%

As shown in Figs. 7 and 8, under identical launch distance conditions, the cylinder pressure greatly affected the launch process, including the take-off speed and overload. The maximum take-off speed of the UAV increases with increasing inflation pressure, and the upward trend of the speed increases. The reason is that, during the launch process, the pneumatic actuator must overcome all external loads. With increasing cylinder pressure, the pneumatic actuator provides a relatively strong force, which increases the take-off speed and overload of the UAV. The key values describing the effect of the changes in cylinder pressure on the launch performance are presented in Table 2.

4.2 Influence of other parameters

We repeated the steps described in Section 3.1 to simulate and analyse the UAV mass, launch angle, cylinder volume, pulley block moment of inertia and cylinder action area. The parameters were changed to study the effect on the dynamic response of the pneumatic launch system, as presented in Table 3.

The results presented in Table 3 show that, during the UAV launching process, the take-off speed and take-off overload of the UAV increased with increasing inflation pressure, volume of the gas cylinder and effective area of the cylinder; i.e., they show a positive correlation, but decreased with increasing mass of the UAV and moment of inertia of the pulley block, revealing a negative correlation.

4.3 Sensitivity analysis of system parameters

Based on the preceding analyses of the effects of key parameters on the launch performance, we conducted a sensitivity analysis of the key parameters, which can efficiently evaluate the effects of their variation on the launch speed and overload. To further explore the impact of the analysed system parameters on the performance of the launch system and lay the foundation for subsequent research on the matching characteristics of the UAV and launcher, the optimal Latin hypercube design method in the Design of Experiments (DOE) component of Isight [19] was used for the analysis [20].

For the sensitivity analysis, the UAV mass, launch angle, moment of inertia of the accelerating pulley block, volume of the gas cylinder, inflation pressure of the gas cylinder and effective area of the cylinder were used as the design variables, and the launch speed and overload as the responses. Thus, the percentage sensitivity is expressed as

$$S_{ri} = \frac{S_i}{\sum_{i=1}^{n_1} |S_i|} \times 100\% \tag{20}$$

$$S_i = \frac{f(x_1, x_2, \dots, x_i + \Delta x_i, \dots, x_n)}{\Delta x_i} - \frac{f(x_1, x_2, \dots, x_i + \Delta x_i, \dots, x_n)}{\Delta x_i} \tag{21}$$

where S_{ri} is the percentage sensitivity, S_i is the sensitivity of each design variable change and n_1 is the total number of design variables.

The results provide a Pareto diagram of the influence of these design variables on the launch speed and overload. A positive, blue value indicates a positive effect, while a negative, red value represents a negative effect. A positive effect shows that the index increases when the design variable is increased, and a negative effect that the index decreases when the design variable is increased. The magnitude of the value indicates the degree of the influence on the system.

As shown in Figs. 9 and 10, the UAV characteristics, the moment of inertia of the pulley block and the inflation pressure of the gas cylinder are the most important parameters that influence the take-off speed and launch overload of the launch system. Increasing the mass or moment of inertia of the UAV has a negative effect on the take-off speed and launch overload, while increasing the pressure has a positive effect.

5.0 Analysis of Matching Characteristics of Pneumatic Launch System

5.1 Analysis of matching characteristics of launch system parameters

According to the parameter sensitivity analysis described in Section 3, it can be concluded that the three key parameters that affect the launch performance are the parameters of the UAV system, the mechanical structure parameters and the parameters of the pneumatic transmission system of the launch system. To study the maximum matching area of the three key parameters under the constraints of the launch take-off safety criterion, according to the relevant safety criteria of UAV launches in literature [21–22], the results can be summarised as follows:

$$\begin{cases} V_{\max} \leq \sqrt{\frac{2T \cos(\alpha + \gamma)}{\rho S_{ref} g(\alpha) \cos(\angle f(\alpha) + \gamma)}} a \\ V_{\min} \geq \frac{-0.5m \sin \gamma + \sqrt{\Delta}}{\rho S_{ref} g(\alpha) \cos(\angle f(\alpha) + \gamma)} \end{cases} \tag{22}$$

$$V_{\min} < V < V_{\max} \tag{23}$$

where

$$\Delta = 0.25m^2 \sin^2 \gamma - 2\rho S_{ref} g(\alpha) \cos(\angle f(\alpha) + \gamma)(T \sin(\alpha + \gamma) - mg) \tag{24}$$

$$\cos \angle f(\alpha) = \frac{0.079\alpha + 0.393}{\sqrt{(0.0036\alpha + 0.024)^2 + (0.079\alpha + 0.393)^2}} \tag{25}$$

$$a \leq 0.5V_{\min} \tag{26}$$

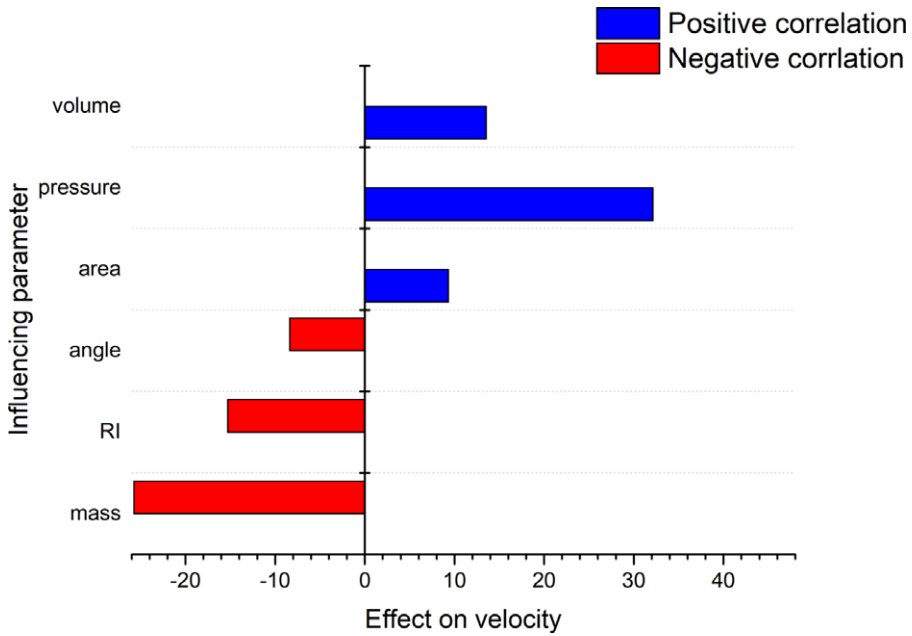


Figure 9. Pareto chart of speed.

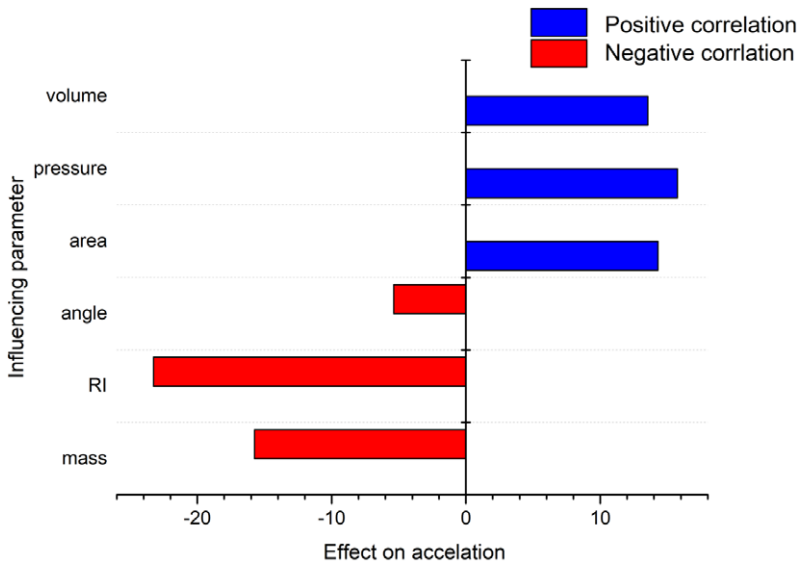


Figure 10. Pareto chart of acceleration.

In these formula, V_{max} and V_{min} are the maximum and minimum speeds of the UAV launch and take-off, respectively, T is the engine thrust, α is the installation angle of the UAV on the launch system, γ is the launch angle, ρ is the standard atmospheric pressure density, S_{ref} is the aircraft wing area and a is the launch overload of the UAV. Hence, the speed range of the UAV launch should satisfy $21m/s < V < 31m/s$, and the launch overload should satisfy $a \leq 10.5g$.

The maximum working pressure of a pneumatic actuator is generally 0.8MPa, and the moment of inertia of pulley blocks should not be excessive due to limitations on their size and weight. Combined

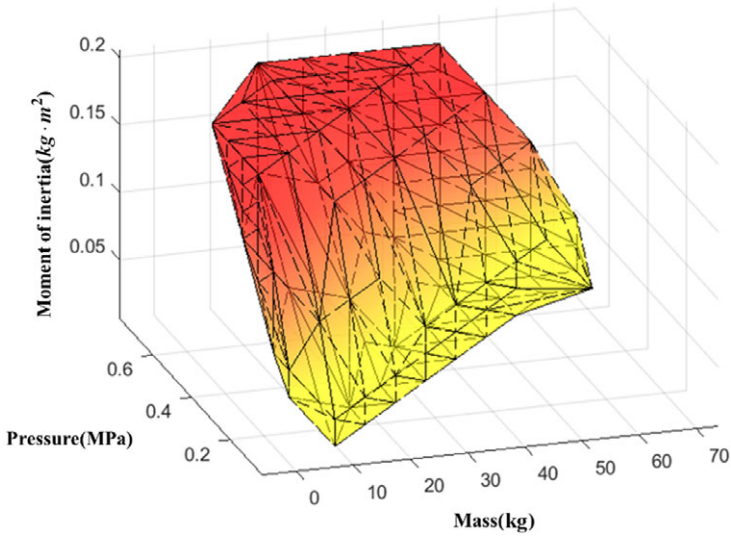


Figure 11. Main UAV launch system parameters.

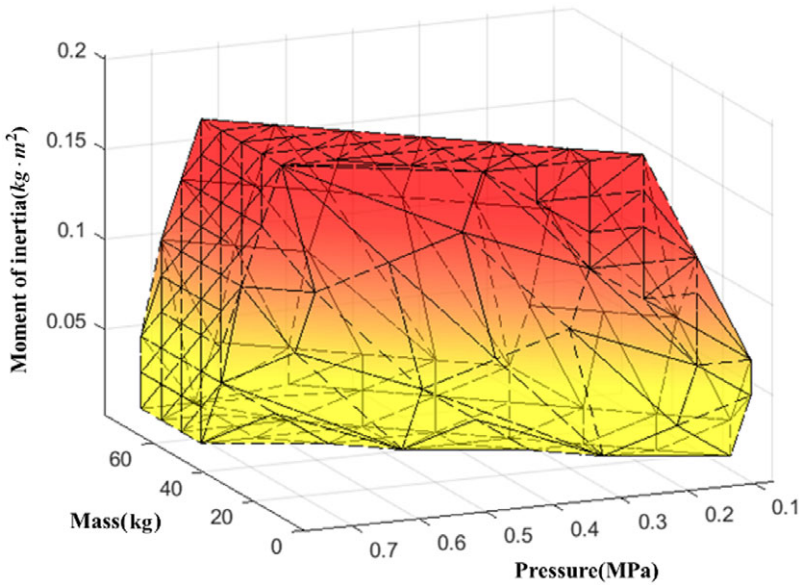


Figure 12. Main UAV launch system parameters.

with engineering experience, the technical index of the launch mass of a UAV is $M = (5 \sim 80)kg$, the working pressure of the pneumatic actuator is $P = (0.1 \sim 0.8)MPa$ and the moment of inertia of the pulley blocks is $kg \cdot m^2$. A step size is adopted to perform the batch simulation. Based on the boundary conditions of the iterative simulation calculation from the safety criterion, a three-dimensional characterisation diagram of the parameter matching value set for the UAV system and pneumatic launch system that satisfies the safety criterion at launch can be obtained; the results are shown in Figs 11–14.

The batch simulation results show that the UAV can be safely launched when the matching values of the system parameters (M, P, RI) are located inside the envelope shown in the figures. A closer parameter matching value corresponds to the light-colour area with higher take-off speed and overload of the UAV.

In addition, Figs 11 and 12 show, that under the safety criteria of the UAV launch take-off speed and overload, the mass M of the UAV increases with a decrease in the rotational inertia I_p of the pulley block

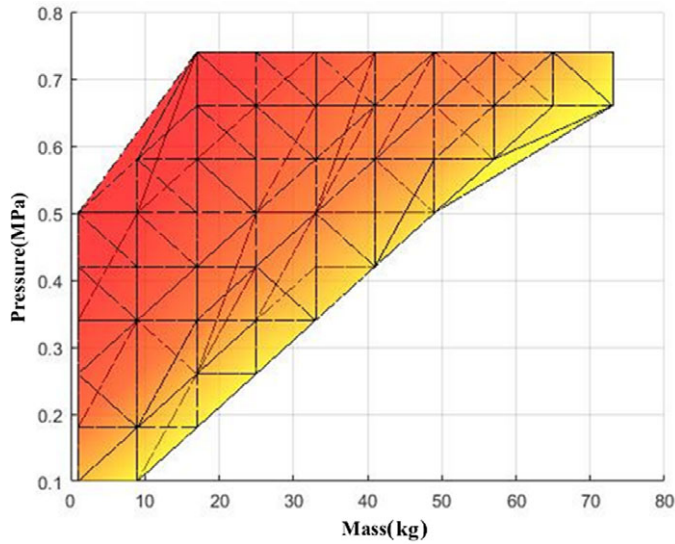


Figure 13. Main UAV launch system parameters.

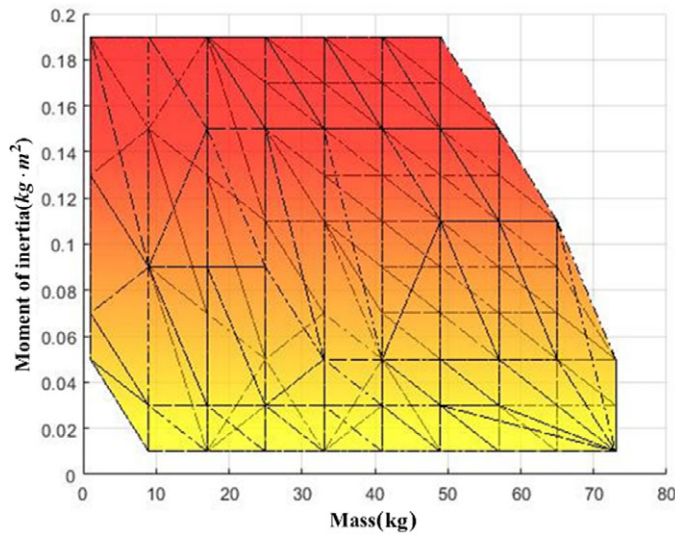


Figure 14. Main UAV launch system parameters.

and an increase in the inflation pressure P of the gas cylinder. Thus, reducing the moment of inertia of the pulley block and increasing the charging pressure of the gas cylinder can improve the maximum take-off mass of the UAV, while also expanding the application range of the pneumatic launch system. In the vertical view shown in Fig. 13, the abscissa represents the range of mass M of the UAV while the ordinate represents the range of the inflation pressure P . When changing the inflation pressure, the range of the UAV mass change increases, indicating that the inflation pressure greatly affects the matching range of the UAV mass. In the right view shown in Fig. 14, changing the moment of inertia of the pulley block I_p hardly affects the UAV mass matching area. Therefore, when top-level parameter matching design is performed for a UAV pneumatic launch system, to enable the launch system to be applied to more massive UAVs, the focus should be on the design and analysis of the inflation pressure.

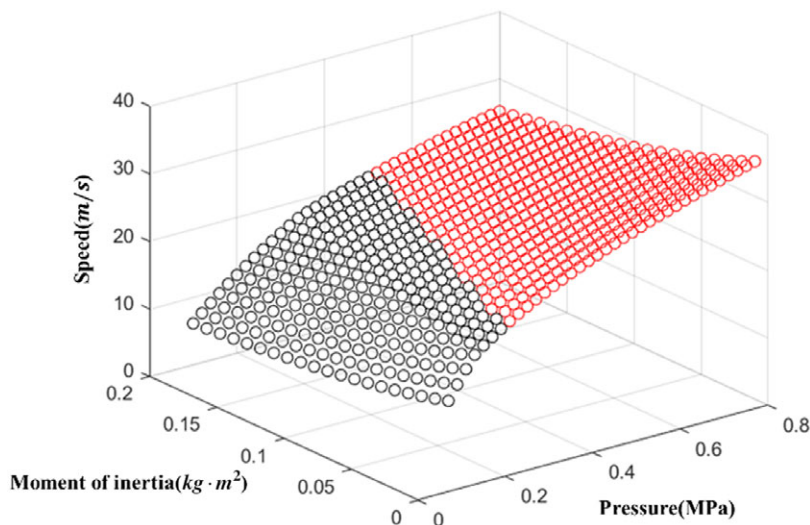


Figure 15. Three-dimensional view of UAV speed response.

6.0 Optimal Design Based on the Influence of Dual Parameters

According to the sensitivity results shown in Figs. 9 and 10, the two parameters with the greatest influence on the dynamic characteristics of the pneumatic launch system are the charging pressure and the moment of inertia of the pulley block. Therefore, the optimised design presented herein is based on only these two parameters while the other parameters such as the launch angle, UAV mass and storage cylinder volume are selected with fixed values. In this paper, the mass of the UAV is 20kg, the volume of the storage cylinder is 80L and the launch angle is 8° . The system parameters of the launch device, including the moment of inertia of the pulley block and the inflation pressure, are considered to analyse in depth the influence of the pneumatic launch system parameters on the launch performance. The dual-parameter response analysis and optimisation design are scrutinised to increase the take-off speed of the UAV, reduce the launch overload and ensure that the pneumatic launch system has the best parameter combination under the given boundary conditions.

We set the inflation pressure to $0.1\text{MPa} \sim 0.8\text{MPa}$ with 0.02 as the step size, and the pulley block moment of inertia to $0.01\text{kg} \cdot \text{m}^2 \sim 0.02\text{kg} \cdot \text{m}^2$ with 0.001 as the step size, for a total of 720 operating conditions. Then, batch simulation calculations were performed on the speed and overload using the mathematical model. We set launch speeds above 21m/s and maximum launch overloads below 10.5g as the red area, which indicates that the resulting parameters satisfy the safety criterion for UAV launch, thus representing a safe launch condition. The results are shown in Figs 15–18.

As shown in Figs 15 and 17, the relationships between the moment of inertia of the pulley block and the inflation pressure of the gas tank on the launch speed and launch overload of the UAV are non-linear. The speed and overload responses are saddle-shaped, and the spatial distributions of the velocity and overload are opposite under the boundary conditions.

The two-dimensional views shown in Figs 16 and 18 illustrate the inflation pressure and moment of inertia under the take-off speed and launch overload distributions. Increasing the pressure or decreasing the moment of inertia will increase the take-off speed but also affect the overload. Hence, when using pneumatic launch systems, the charging pressure of the gas cylinder should be increased while the moment of inertia of the pulley block should be reduced under the condition of the overload requirement.

According to the preceding analysis of the boundary conditions for speed and overload, achieving the maximum speed and minimum overload was set as the optimisation goal, and the inflation pressure of the gas cylinder ($0.1\text{MPa} \sim 0.8\text{MPa}$) and moment of inertia of the pulley block ($0.01\text{kg} \cdot \text{m}^2 \sim 0.02\text{kg} \cdot \text{m}^2$) were optimised based on the multi-island genetic algorithm [23]. The model is shown in Fig. 19.

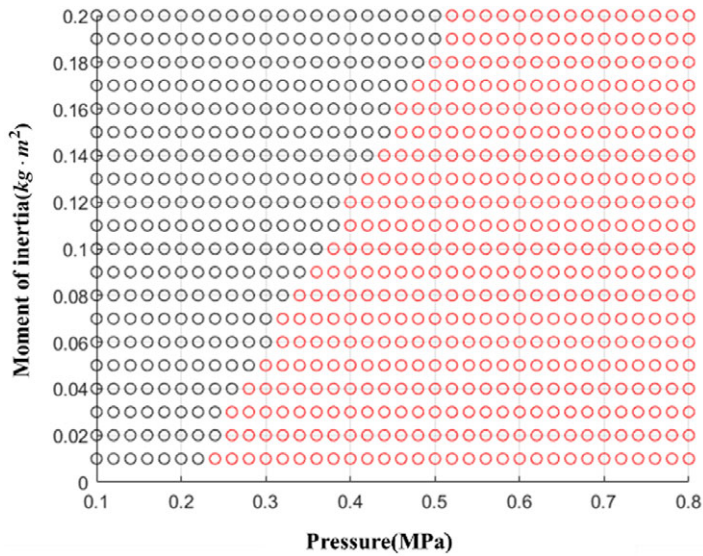


Figure 16. Two-dimensional view of UAV speed response.

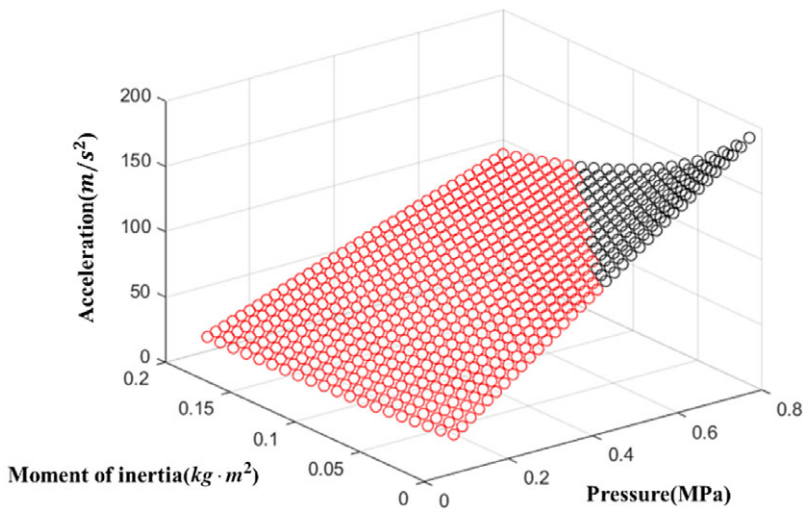


Figure 17. Three-dimensional view of UAV acceleration response.

Table 4. System parameter optimisation results

Input	Value	Output	Value
Pressure	0.42MPa	Speed	25.26m/s
Moment of inertia	0.028 kg·m ²	Acceleration	9.16g

The final optimisation results are shown in Table 4 and Figs 20 and 21.

As shown in Table 4, when the pressure of the air cylinder is 0.42MPa and the moment of inertia of the pulley block is 0.028kg·m², the maximum speed is 25.26 m/s, and the largest overload is 9.16g, which can be considered a relatively ideal parameter combination in this study.

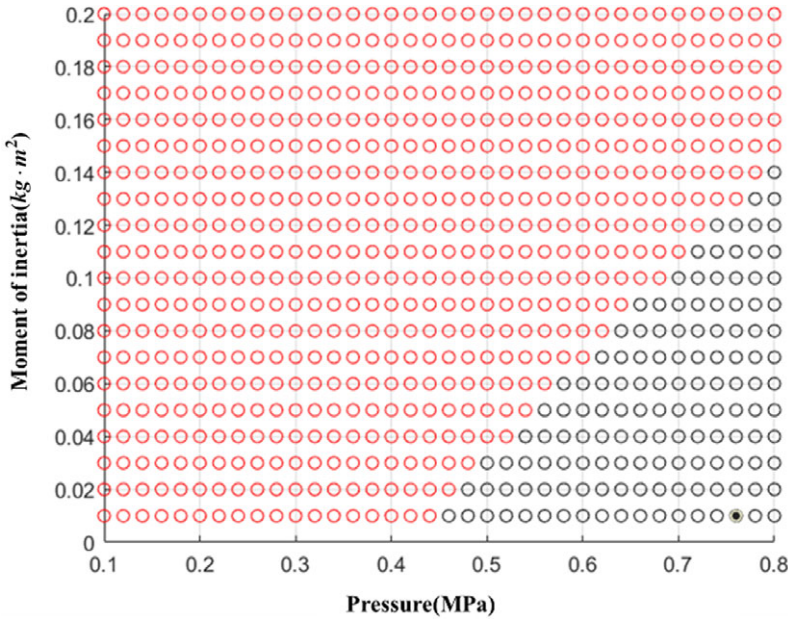


Figure 18. Two-dimensional view of UAV acceleration response.

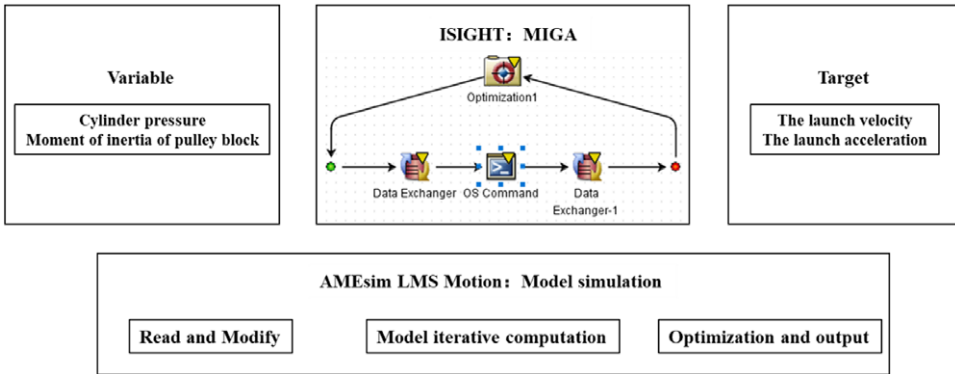


Figure 19. Schematic diagram of optimisation model.

7.0 Conclusions

A dynamic model for a UAV pneumatic launch system was established based on co-simulation, considering the coupling characteristics of the mechanical structure of the UAV and the transmission system, and verified by testing. Based on this model, we clarified the effects of the key parameters, including the mass of the UAV, moment of inertia of the accelerating pulley block and inflation pressure of the gas cylinder, on the performance of the UAV pneumatic launch. A new method for the parameter matching characteristics between the UAV and launch system based on batch simulation is proposed to analyse the influence of the system parameters of the UAV launch process on the launch performance and optimise the design. The results of this analysis can be summarised as follows:

- (1) The comparisons between the simulation and test results show that the co-simulation model demonstrates a favourable correlation with the real situation. Thus, the co-simulation method offers many benefits for the analysis of pneumatic launch characteristics.

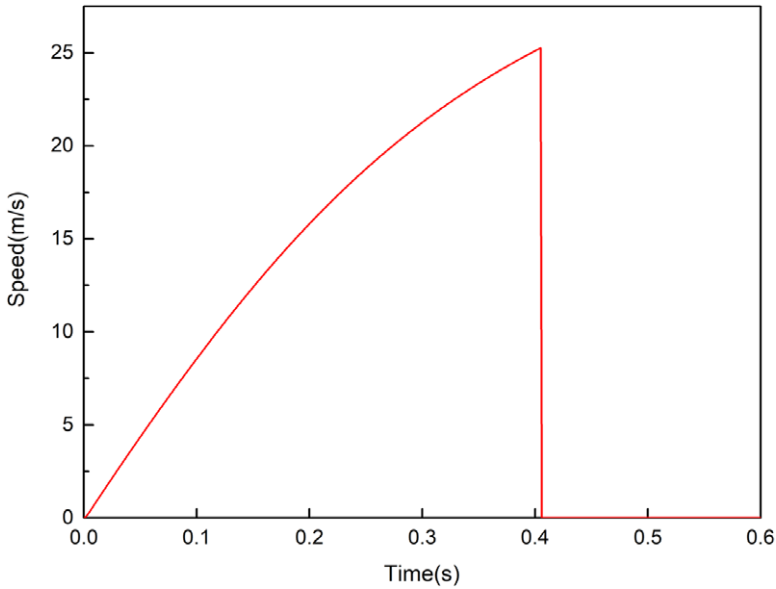


Figure 20. Optimised take-off speed.

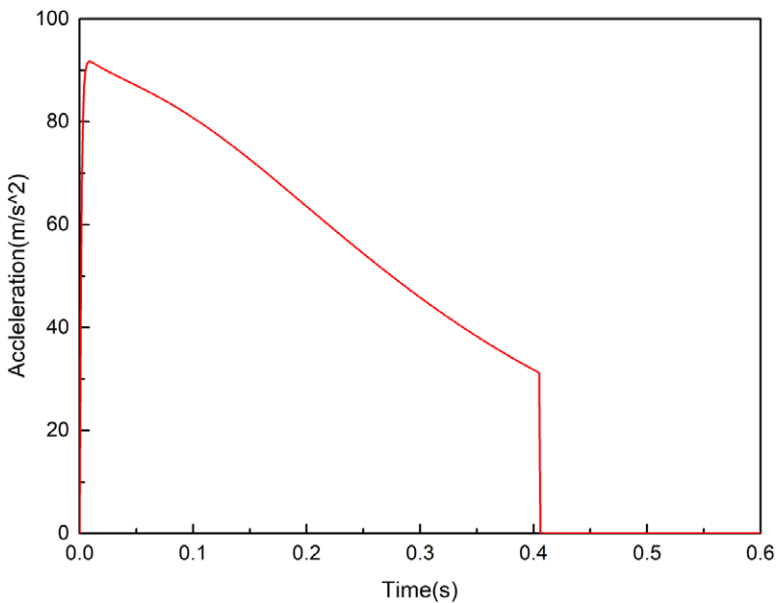


Figure 21. Optimised overload.

- (2) The sensitivity analysis shows that the UAV mass, pulley block rotational inertia and cylinder inflation pressure have a relatively greater impact than other factors on the UAV pneumatic launch performance. The UAV mass and pulley block rotational inertia have a negative correlation with the launch speed and overload, while the inflation pressure of the gas cylinder is positively correlated.
- (3) When the cylinder inflation pressure is increased, the driving force increases. The take-off speed and launch overload relatively increase in the launch process. When the pulley block rotational inertia is increased, the energy consumed by the rotation of the pulley block increases, and the

friction between the pulley and rope increases, which reduces the launch take-off speed and overload. When the mass of the UAV is increased, the kinetic energy of the pneumatic launch decreases while the take-off speed and overload decrease sharply.

- (4) The matching envelope of the UAV system and pneumatic launch system takes the UAV launch take-off speed and launch overload as the boundary conditions and is closed by the UAV mass, pulley block moment of inertia and gas cylinder inflation pressure curves. The maximum launch mass that the pneumatic launch system allows is determined by the air cylinder inflation pressure and pulley block moment of inertia. In the matching value set, with increasing inflation pressure and decreasing pulley block moment of inertia, the UAV mass distribution range increases.
- (5) Three parameters are optimised by using a multi-island genetic algorithm, and the optimal solution is found in 500 iterations. It is suggested that the cylinder inflation pressure should be set to 0.42, and the pulley block rotational inertia to 0.028. Under this condition, both the take-off speed and launch overload will be effective.

References

- [1] DA FORM 2397-U. Unmanned Aircraft System Accident Report (UASAR).
- [2] Siddiqui B.A., Rahman H.U., Kumar C., Solen M.A. and Bashir U.D. Computer Aided Modeling and Simulation of Pneumatic U.A.V. Catapult Mechanism. 7th International Mechanical Engineering Congress. 2017, 24–25.
- [3] The Editors of “The Whole UAVs in the World”. The Whole UAVs in the World. Beijing: Aviation Industry Press, 2004:288–296. (in Chinese)
- [4] Kondratiuk, M. and Ambroziak, L. Design and dynamics of kinetic launcher for unmanned aerial vehicles. *Appl. Sciences*, 2020, **10**, 2949. doi: [10.3390/app10082949](https://doi.org/10.3390/app10082949).
- [5] Jastrzebski, G. Impact of opening time of the take-off pneumatic launcher main valve on take-off pressure losses, *J. KONES*, 2016, **23**, (4), 175–182.
- [6] Szczepaniak, P. and Jozko, M. (2017). Research of Pneumatic Distributors for Launcher of Unmanned Aerial Vehicle (UAV). *J. KONBiN*, **43**, 249–276. doi: [10.1515/jok-2017-0049](https://doi.org/10.1515/jok-2017-0049).
- [7] Min, H., Cheng, H. and Jinhua, P. Dynamic Analysis and Optimization of Pneumatic Wedge-Shaped Launcher for UAV. *Trans. Nanjing Univ. Aeronaut. Astronaut.*, 2018, (5), 866–873.
- [8] Xiao Long, L., Shenggang M.. Simulation research on launch performance of UAV pneumatic launch system. *J. Zhengzhou Univ. (Eng. Sci.)*, 2013, **34**, (5), pp 56–58.
- [9] Khadr, A., Houidi, A. and Romdhane, L. Development of Co-simulation Environment with ADAMS/Simulink to Study Maneuvers of a Scooter, Berlin, Heidelberg, 2013. Springer Berlin Heidelberg, 2013.
- [10] Zheng D., Ren L., Wu Y. and Liu J. Research on Multi-physical Modeling and Co-simulation of Aircraft, Cham. Proceedings of the 16th Chinese CAE Engineering Analysis Technology Annual Conference, 2020, 5.
- [11] Liu, Z., Zhan, H. and Wang, S. Parameter Matching Characteristics and Safe Set of Carrier Aircraft during Landing Process. 7th Asia-Pacific International Symposium on Aerospace Technology, 2015.
- [12] Liu, X., Xu, D. and Wang, L. Match characteristics of aircraft-carrier parameters during catapult takeoff of carrier-based aircraft. *Acta Aeronaut. Astronaut. Sin.*, 2010, **31**, (1), pp 102–108.
- [13] Wei, L., Xiaoping, M., Ming, Z. and Yang, H. Dynamic simulation and optimization of UAV pneumatic launching. *J. Northwestern Polytech. Univ.*, 2014, **32**, (6), 865–871.
- [14] Li Rui., Pei Jinhua.. Dynamic numerical simulation of the pneumatic and hydraulic launching of UAV. *J. Mech. Eng.*, 2011, **47**, (8), 183–190(in Chinese).
- [15] Aquilen-Gomez, E. and Lara-Lopez, A. dynamic of a pneumatic system modeling simulation and experiments. *Int. J. Robot. Autom.*, 1999, **14**, (1), pp 39–43.
- [16] Jian Fan, L. Pneumatic Transmission System Dynamics, South China University of Technology Press, 1991.
- [17] LMS Imagine. Lab AMESim: AMESim Users’ Guide. LMS International. 2015, Belgium.
- [18] LMS Virtual. Lab Motion: VL Motion Users’ Guide. LMS International. 2015, Belgium.
- [19] Simulia Isight: ISIGHT Users’ Guide. Dassault Systems, 2016, Paris.
- [20] Munk, D.J., Auld, D.J., Steven, G.P. and Vio, G.A. On the benefits of applying topology optimization to structural design of aircraft components. *Struct. Multidisc. Optim.*, 2019, **60**, (3), pp 1245–1266.
- [21] Lucas, C.B. Catapult criteria for a carrier based airplane. AD702814, 1968.
- [22] Li, K. The Research of Ejection Takeoff and Skyhook Technology of Small UAVs, Nanjing University of Aeronautics and Astronautics, 2019.
- [23] Chen, H., Fang, X., Zhang, Z., Xie, X., Nie, H. and Wei, X. Parameter optimisation of a carrier-based UAV drawbar based on strain fatigue analysis, *Aeronaut. J.*, 1–20. doi: [10.1017/aer.2021.1](https://doi.org/10.1017/aer.2021.1)